Characterization of the solid matrix in the meniscus of the human knee joint by using scanning electron microscopy SEM

Gilberto Piña Piña[1], Jorge Antonio Ascencio Gutiérrez[2], Enrique Bernardino Sánchez Diaz[1]
[1]Technological Institute of Toluca, [2]Institute of Physical Sciences UNAM,
gpinap@toluca.tecnm.mx, ascencio@fis.unam.mx, esanchezd@toluca.tecnm.mx

http://dx.doi.org/10.37057/2433-202x
Issue DOI http://dx.doi.org/10.37057/2433-202x-209-2021-2
Article DOI http://dx.doi.org/10.5281/zenodo.5150145

Abstract:

The study of the solid matrix of the human knee joint meniscus using scanning electronic microscopy (SEM) techniques, will identify the anatomical physiological constituent elements of it. The basic elements of analysis are: the orientation of collagen fibers at different depths of the thickness of the meniscus, the physiological relationship between collagen and proteoglycan during the compression of the meniscus, the cells of the meniscus of the knee, channels of diffusion of nutrients in avascular areas of meniscal tissue, the tensions to which these joints are subjected in the mechanics of locomotion.

Keywords: Scanning Electronic Microscopy, Meniscus, Collagen fibers, Diffusion.

The importance of the preparation of samples is an important factor to obtain reliable results. To ensure the above the Watanabe´s method was used, that was modified by Pirela and Col. On the other hand, the pretreatment prior to be observed through the SEM must be done with the standards recommended in order not to contaminate the samples. Analyses of micrographs are from the histological viewpoint, according to the resistance of the tissue.

Sampling

One of the specimens of the human knee meniscus used in this research was provided by the Forensic Medicine Institution of the Universidad Veracruzana and corresponds to a person of the male sex of approximately 65 years old; another sample, belonged to a young 26 years old athlete, which had been previously diagnosed with torn medial meniscus, through a study of magnetic resonance and followed this was practiced with a partial menisectomy of the damaged meniscus. The first sample was

Preserved in 10% formalin while the second one remained in absolute alcohol. Both samples were processed at the Biotechnology Institute and the Physical Sciences Institute of the UNAM.

Processing of the sample for transmission electron microscopy.

The processing of the samples was done per the Watanabe´s technical, modified by Pirela and Col. A portion of the specimen was used to study regions of the meniscus in cross-sections, for TEM-Transmission electron microscopy, by applying resins EPON / LRW; the rest of the meniscus was processed for scanning electron microscopy SEM.

Preparation of the sample for transmission electron microscopy.

Meniscal samples were cut into pieces of (1.0 mm) approximately to its fixation with GTA 6% cacodylate 0.1 M, PH 7.2 and kept at 4 ℃ for 6 days. At the end of this stage, fixed meniscus blocks were washed (2 x 15 min) with buffer cacodylate 0.1 M, PH 7.2. We then proceeded to remove this solution and wash small pieces of meniscus in cacodylate buffer. The samples were dehydrated by upward gradients of ethanol (70, 75, 085, 95 and 100) % for 15 minutes per sample. Samples were separated to include samples of meniscus in two different resins.

Preparation for inclusion in resin EPON

Jump to an agent that facilitates the penetration of the resin, in this case the blocks were moved to (OP) Propylene oxide, using two changes (15 min); Mixtures of resin EPON and propylene oxide were done in the proportions and times indicated in the table 1, to get infiltration of the resin in the sample adequately.

Table 1: Proportion of resin EPON and propylene oxide at different times.

Propylene Oxide	EPON	Time
2	1	3 hours
1	1	1 night
1	0	1 hour

The last change with resin EPON pure are used by placing the samples in molds. Then, the molds are carried with the sample to a convection oven and dried at a temperature of 60 ℃ for one night.

Five pairs of cross-sections laminar fine (60 nm) were practiced; they were mounted in racks of copper to 200 mesh with gold and carbon-reinforced. The cuts were made with a diamond blade through an ultramicrotome brand Porter Blue MT-2, the samples were contrasted by treatment of uranyl acetate 2% for (30 min) in a humid chamber and lead citrate during 15 min and were left to dry for a few hours. Once contrasted the samples were observed with an electron microscope.

Preparation for inclusion in resin LRW

After dehydration, the mixture is passed to resine LRW, to facilitate this penetration, absolute ethanol was added in the proportions and times indicated in the table 2.

Table 2: LRW Resine and Ethanol proportions at different times.

Ethanol	LRW	Time
2	1	3 hours
1	1	3 hours
2	1	3 hours
0	1	1 night

The last change with LRW is used by placing the samples in a mold, it is then polymerized cold by using LUV for 2 days.

Scannin Electron Microscopy SEM

Upward gradients of ethanol (70, 75, 85, 95 and 100) % for 15 minutes for each one, samples are kept in absolute ethanol and finally change to oxide from propylene (2 changes of 15 minutes).

Samples preparations to observe for SEM.

Signs of low electrical conductivity are a buildup of charge on the surface when they are observed in a scanning microscope. This buildup, known as polarization, is capable of distorting the image generated by the secondary electrons and they can generate heat damage (burning of the sample). Some of the techniques that reduce or eliminate the problem are. (a) decrease the energy of the electron beam, b) deposits on the surface conductive films and c) increase the conductivity of the sample by mixing some conductor in it.

The second method is used to a greater degree in mineral specimens, semiconductors and biological samples. This is done on equipment that can evaporate the metal or carbon arc and condense on the sample. Film evaporation methods include: thermal evaporation, electric arc and under conditions of

high vacuum electron beam (10-7 - 10-3 torr). Thermal evaporation metals include: Pt, Cr, Al, Au, Cu, etc.).

Fix samples with GTA 6% cacodylate 0.1 M, ph 7.2 and kept at 4 °C for 6 days. Wash (2x 15 min) in buffer cacodylate 0.1 M, PH 7.2. Then fix in OsO cacodylate GTA 6% for 1 hour. Wash in the cacodylate buffer to retire the osmium oxide.

The samples were dried and metallized with a layer of gold/palladium for 30 seconds of exposure, to be observed by scanning electron microscope (micro probe) Jeol - 6400.

Analysis of micrographs SEM

In Figure 1 there is a histological section, which is in contact with the surface of a stainless steel whose background is completely dark Cap. In this specimen, we can appreciate the side face of the meniscus (1), the top part (2) and (3) cut in cross-section with diamond knife. Micrographs were cross, top and side cut for analysis by SEM.

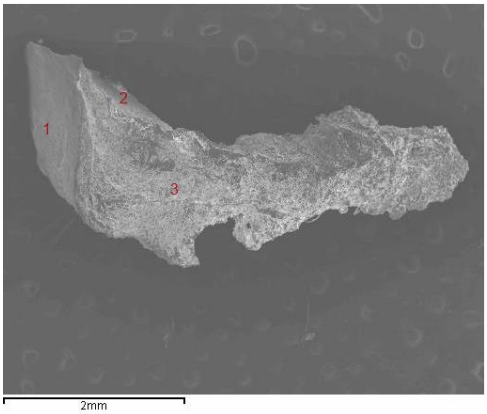

Figure 1: Specimen of human knee meniscus: 1 side, 2 upper face, 3 sided in cross section.

In the figure 2, it shows part of the face upper intact. This micrograph shows a surface with deeper than the side undulations. Unlike of this, the ridges are much higher, which allows to observe the direction of collagen. Clearly, what is seen on the upper surface, the collagen is oriented radially and longitudinally, intertwining in these two directions.

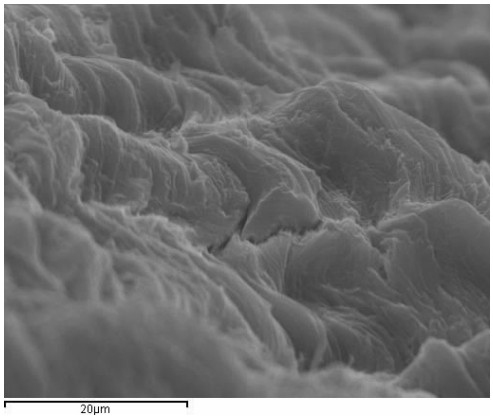

Figure 2: Top of the meniscus, 1000 X.

Following micrographs are of cross-sections of the meniscus. Each one is made with different extensions. From these, important findings are removed. Figure 3 corresponds to the cross-section of the meniscus, from which you can see inside radial directions of collagen in the third layer of depth. Also shows the collagen fibers, which appear as strands in different thicknesses. In the central part there is a hole of this specimen, which is one of the lakes that are nothing more than the interstitial spaces. On the other hand, different thicknesses of collagen fibers can be seen more clearly.

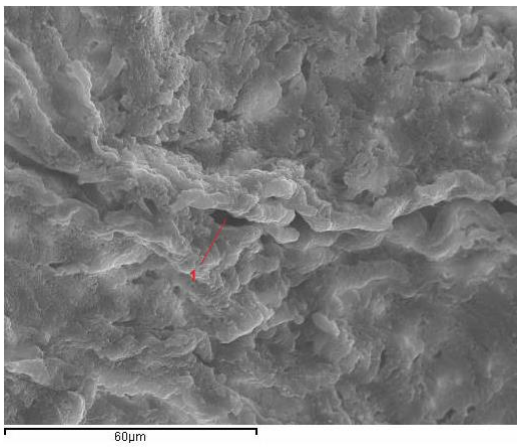

Figure 3: Cut in cross section of the meniscus, 1000 X.

In figure 4, a bright thin fibril identified is seen at the edges of the collagen fibers with the number 4, which corresponds to the proteoglycan. Proteoglycans are hydrophilic molecules, negatively charged that could hold water above 50 times their body weight. The forces of the collagen fibers (3) in the interior of the meniscus portion froze these proteoglycans. During compression, they slowly dissipate

the trapped water and hereby help to constrain the compressive forces, the fluid is loaded positively, the fluid is drawn into the interstitial spaces (2) when compressive

loads are applied concerning the meniscus. The positive charges of the flow are attracted by the negative charges of the proteoglycans. The micrograph shows a deep area of the meniscus since it only consists of spherical chondrocytes, characteristic of the deep area. When age increases, changes in the vasculature, which include a decrease in vascular peripheral and central margin of the meniscus the number of cells of the meniscus decreases considerably, is by this reason we find few cells in the micrograph. At the bottom of the ponds we observe collagen oriented in a perpendicular direction (5), compared to collagen, which is identified by (3).

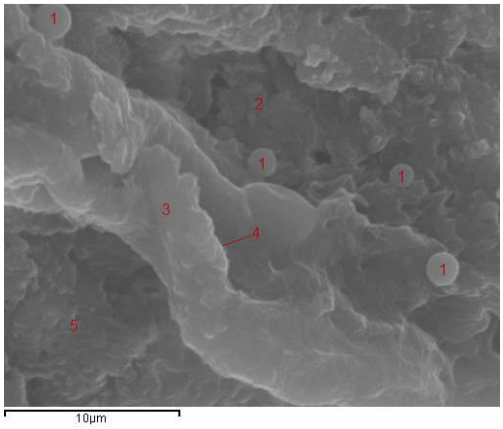

Figure 4: Assessment of collagen, proteoglycans and chondrocytes, lagoons, 2000 X.

Figure 5 shows the surface, consistent coat of fine fibers of collagen woven mesh, which is covered by the thin and compact surface layer whose Collagen fibers are aligned irregularly shaped In the middle layer, the collagen fibers are arranged in bundles of 50-150 nm and they are oriented circumferentially, parallel to the periphery of the meniscus, these seem to be continuous with the anterior and posterior ligaments in the middle layer horns. Also found, are Collagen fibers oriented radially, interlacing with fibers that run in a circumferential manner. Finally see that the fibers of the deep layer, the collagen are organized in a circumferential manner.

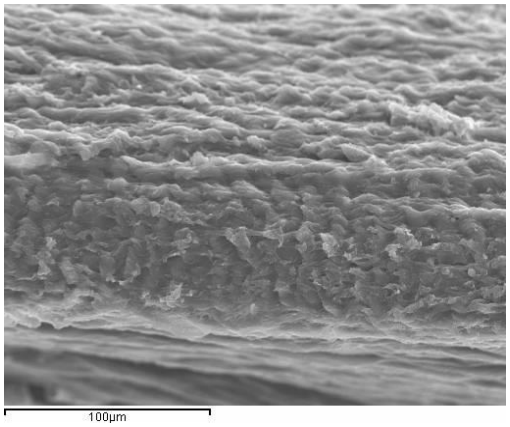

Figura 5: Organization of collagen fibers at different depths.

Figure 6 shows a microscopic channel that passes from the surface to the deep area within the fabric of the meniscus. The diameter of this is of the order of 10 micrometers. In the deep area, the tissue of the meniscus is avascular; This particular feature causes lesions in this area not to heal in the same way as on the surface and at the edges of the meniscus. The nutrition of the meniscus in the deep area is through diffusion; this is done through the channels that we see in Figure 6.

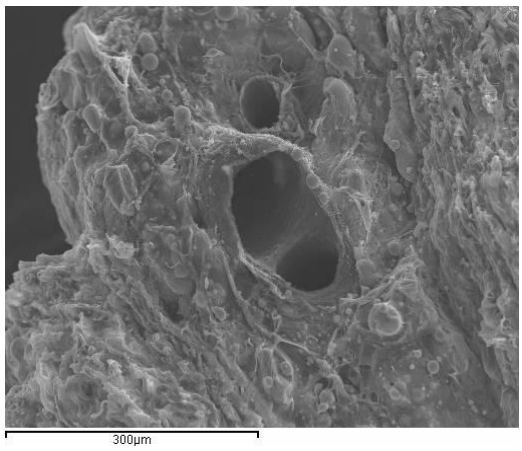

Figura 6: Diffusion channel, through which the deep area of the meniscus is nourished.

Figure 7 shows at a glance the tear since there are two different forms of chondrocytes which correspond to different zones of the same depth in its proximity. These types can be identified through different levels of scanning electron microscopy. In the surface area, the chondrocytes tend to be oval, while in the deep zone they are round. Scattered populations of chondrocytes were found. These cells are responsible for the synthesis, maintenance and repair of the intracellular matrix.

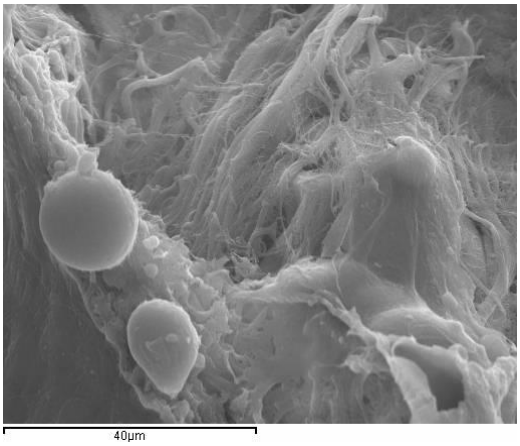

Figure 7: Meniscus tear, which is appreciated by the presence of differently condrositos.

Also we can see in Figure 7 the variation in the diameter of the collagen fibers. THE addressing of these fibers is erratic because it is of a tear, which modified the addresses of the fibers, the position of the chondrocytes and in general all the elements of the array.

Conclusions

1. The strength of the collagen fibers in the interior of the meniscus portion comes from frozen proteoglycans. During compression, they slowly dissipate the trapped water and hereby help to constrain the compressive forces.

2. Based on this study of electron microscopy, it was found that there are three different layers in the human knee meniscus. In the microstructure of collagen meniscus, the deep inner area of this mainly has fibers oriented circumferentially. The fibers are oriented in bundles of 20 to 150 micrometers in diameter and continue in the joints of the anterior and posterior horns of the meniscus. The inner area next to the surface of the meniscus, contains mostly fibers oriented both radially and longitudinally, approximately 20 to 130 micrometers in diameter.

Bibliography

Agoram, B. and V. H. Barocas. Coupled macroscopic and microscopic scale modeling of fibrillar tissues and tissue equivalents. J. Biomech. Eng. 123:362–369, 2001.

Ahlfors, J. E. and K. L. Billiar. Biomechanical and biochemical characteristics of a human fibroblast-produced and remodeled matrix. Biomaterials 28:2183–2191, 2007.

Alini,M.,W. Li, P. Markovic, M. Aebi, R.C. Spiro, and P.J. Roughley. The potential and limitation of a cell-seeded collagen/hyaluronan scaffold to engineer an intervertebral disc-like matrix. Spine 28:446–54, 2003.

Awad, H. A., D. L. Butler, M. T. Harris, R. E. Ibrahim, Y. Wu, R. G. Young, S. Kadiyala, and G. P. Boivin. In vitro characterization of mesenchymal stem cell-seeded collagen scaffolds for tendon repair: effects of initial seeding density on contraction kinetics. J. Biomed. Mater. Res. 51:233–240, 2000.

Barocas, V. H., T. S. Girton, and R. T. Tranquillo. Engineered alignment in media equivalents: magnetic prealignment and mandrel compaction. J. Biomech. Eng. 120: 660–666, 1998.

Barocas, V. H., A. G. Moon, and R. T. Tranquillo. The fibroblast-populated collagen microsphere assay of cell traction force–Part 2: Measurement of the cell traction parameter. J. Biomech. Eng. 117:161–170, 1995.

Barocas, V. H. and R. T. Tranquillo. An anisotropic biphasic theory of tissue-equivalent mechanics: the interplay among cell traction, fibrillar network deformation, fibril alignment, and cell contact guidance. J. Biomech. Eng. 119:137–145, 1997a.

Barocas, V. H. and R. T. Tranquillo. A finite element solution for the anisotropic biphasic theory of tissue-equivalent mechanics: the effect of contact guidance on isometric cell traction measurement. J. Biomech. Eng. 119:261–268, 1997b.

Bell, E., H. P. Ehrlich, D. J. Buttle, and T. Nakatsuji. Living tissue formed in vitro and accepted as skin-equivalent tissue of full thickness. Science 211:1052–1054, 1981a.

Bell, E., H. P. Ehrlich, S. Sher, C. Merrill, R. Sarber, B. Hull, T. Nakatsuji, D. Church, and D. J. Buttle. Development and use of a living skin equivalent. Plast. Reconstr. Surg. 67:386–392, 1981b.

Bell, E., B. Ivarsson, and C.Merrill. Production of a tissue-like structure by contraction of collagen lattices by human fibroblasts of different proliferative potential in vitro. Proc Natl Acad Sci U S A 76:1274–8., 1979.

Bellows, C. G., A. H. Melcher, and J. E. Aubin. Association between tension and orientation of periodontal ligament fibroblasts and exogenous collagen fibres in collagen gels in vitro. J. Cell. Sci. 58:125–138, 1982.

Bellows, C. G., A. H. Melcher, and J. E. Aubin. Contraction and organization of collagen gels by cells cultured from periodontal ligament, gingiva and bone suggest functional differences between cell types. J. Cell. Sci. 50:299–314, 1981.

Berglund, J. D., R. M. Nerem, and A. Sambanis. Viscoelastic testing methodologies for tissue engineered blood vessels. J. Biomech. Eng. 127:1176–1184, 2005.

Berry, C. C., J. C. Shelton, D. L. Bader, and D. A. Lee. Influence of external uniaxial cyclic strain on oriented fibroblast-seeded collagen gels. Tissue Eng. 9:613–624, 2003.

Billiar, K. L., A. M. Throm, and M. T. Frey. Biaxial failure properties of planar living tissue equivalents. J. Biomed. Mater. Res. A. 73:182–191, 2005.

Breuls, R. G., B. G. Sengers, C. W. Oomens, C. V. Bouten, and F. P. Baaijens. Predicting local cell deformations in engineered tissue constructs: a multilevel finite element approach. J. Biomech. Eng. 124:198–207, 2002.